Available online at www.HighTechJournal.org

HighTech and Innovation Journal

ISSN: 2723-9535

Vol. 7, No. 2, June, 2026

Spatiotemporal Patterns and Driving Factors of Soil Organic Carbon Content: A Case Study from a Montane Region

Liang Chen [1*]

[1] *School of Tourism, Xinyang Normal University, Xinyang 464000, China.*

Received 22 September 2025; Revised 26 April 2026; Accepted 11 May 2026; Published 01 June 2026

Abstract

A comprehensive grasp of the vertical distribution profiles of soil organic carbon (SOC) and its underlying governing mechanisms is fundamental to assessing terrestrial carbon stocks. Research efforts in mountain ecosystems, however, frequently fall short in providing depth-resolved analysis. This study investigated the spatial patterns and dominant drivers of SOC content across the full 0–200 cm soil profile in the Dabie Mountain Area (DMA), a subtropical montane region in central China. By utilizing high-resolution (250 m) SOC data and multi-source environmental variables for topography, climate, and soil properties, we employed hots pot analysis (*Getis-Ord Gi**) and the geographical detector model to quantify spatial clustering and identify key influencing factors across six depth intervals in the DMA. The results showed that SOC content decreases exponentially with depth, with the surface 0–5 cm layer containing the highest concentration. A distinct shift in spatial organization occurred at an approximate depth of 60 cm: surface layers (0–60 cm) exhibited strong, clustered patterns (hot spots and cold spots), whereas deeper layers (>60 cm) transitioned to a more dispersed and spatially homogeneous distribution. Factor detection identified elevation and soil bulk density (SBD) as the most influential factors overall. More importantly, interaction detection revealed a depth-dependent transition in the dominant controlling complexes. In surface soils (0–15 cm), SOC heterogeneity was primarily governed by the interaction between topography (elevation) and soil properties (pH and SBD). In contrast, within the subsoil (15–200 cm), the interaction between climatic factors (temperature, precipitation) and soil properties (pH, SBD) became dominant. These findings demonstrated a fundamental shift from a topo-edaphic control regime in surface layers to a climate-edaphic control regime in deeper layers. This study provided a novel, three-dimensional perspective on SOC storage in mountains, highlighting the necessity of depth-resolved analyses for accurate carbon accounting and for formulating stratified land management strategies aimed at soil carbon conservation.

Keywords: Distribution Pattern; Soil Depth; Driver Detection; Soil Organic Carbon.

1. Introduction

Soil organic carbon (SOC) constitutes a critical and dynamic component of the global carbon cycle. Its storage and stability fundamentally regulate atmospheric CO_2 concentrations, soil health, and ecosystem functioning [1, 2]. Consequently, accurately quantifying the spatial distribution of SOC and identifying its dominant environmental drivers are of paramount importance for predicting terrestrial carbon-climate feedbacks and guiding sustainable land use policies [3, 4]. This undertaking proves especially challenging in mountainous regions, where steep topographic gradients amplify environmental heterogeneity, driving rapid changes in microclimate, soil formation, and vegetation [5, 6]. Although the general factors influencing SOC, such as climate [7], topography [8], soil properties [7, 9], and land cover [8, 10], are well-recognized, their relative importance, interactive effects, and especially their shifting roles with

* Corresponding author: chenliang14@mails.ucas.ac.cn

https://doi.org/10.28991/HIJ-2026-07-02-05

increasing soil depth remain inadequately understood at the scale of entire mountain systems. This knowledge gap contributes substantially to uncertainty in regional carbon accounting [5].

Advances in recent literature have enhanced our understanding of SOC drivers via high-resolution mapping and sophisticated statistical models [11, 12]. Investigations across various landscapes repeatedly underscore the scale- and location-dependent nature of these controls [13-15]. To illustrate, large-scale assessments in Eastern Australia often identify climatic variables like temperature and precipitation as primary drivers [16]. On the other hand, finer-scale studies on agricultural or forested hillslopes commonly find terrain attributes (elevation, slope) and soil physicochemical properties (texture, pH, bulk density) to be more influential [17, 18]. Notably, the geographical detector model and its combination with machine learning techniques (e.g., geographical detector-based stratified regression kriging (GD-SRK)) have demonstrated considerable utility in deciphering the non-linear and interactive effects of these factors, moving beyond simple correlation analyses [19, 20]. A persistent and major shortcoming in the literature, however, is its overwhelming focus on surface soils (0-30 cm), even though deep soil layers (>30 cm) are known to store more than half of the global soil carbon stock [21]. This surface-centric focus inhibits a holistic understanding of the soil carbon profile. Emerging studies are now starting to explore this vertical dimension, hinting at a potential change in dominant controls with depth. For example, surface SOC might be more sensitive to climatic and biotic drivers [22, 23], whereas deeper SOC stability could be more strongly governed by mineralogical protection and geochemical factors [24, 25]. Nevertheless, comprehensive studies that systematically evaluate a complete set of potential drivers—topographic, climatic, edaphic, and land cover—over a continuous deep soil profile (e.g., 0-200 cm) within a single, heterogeneous mountain system are still strikingly rare.

The Dabie Mountain Area (DMA) in central China offers an ideal and pressing setting to address these linked knowledge gaps. This area is not just an under-studied location but also a critical ecological zone featuring complex, dissected topography, a transitional climate, and diverse soil types and land uses that ranging from forests to agriculture [26-28]. This configuration creates a pronounced and tightly coupled spatial gradient for all key SOC-forming factors, effectively making it a natural laboratory to investigate their interactions. The ecological vulnerability of the DMA further highlights the practical importance of understanding its soil carbon dynamics [29]. While previous localized studies in the DMA have provided insights into forest SOC accumulation or surface soil-topography relationships, they are fundamentally insufficient [27, 28, 30]. To date, no research has successfully merged high-resolution, spatially continuous data for SOC and its potential drivers across the entire 0-200 cm profile for the whole of the DMA. As a result, critical questions persist: (1) In what manner do the spatial distribution and clustering patterns (hot spots/cold spots) of SOC evolve vertically? (2) How does the individual and, more critically, the interactive impact of terrain, climate, soil properties, and land cover on SOC heterogeneity evolve from the surface to deep layers? Answering these questions is crucial to advancing from a fragmented toward a mechanistic, three-dimensional understanding of SOC storage in montane ecosystems.

To address these deficiencies, this study leverages a high-resolution (250 m) SOC dataset covering 0-200 cm depth, combined with multi-source environmental data, to pursue three key aims: (1) to characterize the spatial and vertical distribution patterns of SOC content throughout the DMA; (2) to delineate statistically significant spatial clusters (hot spots and cold spots) of SOC at different soil depths using *Getis-Ord Gi** analysis; and (3) to measure and contrast the individual and interactive effects of topographic, meteorological, soil, and land cover factors on SOC spatial heterogeneity at every depth interval by applying the geographical detector model. Our research provides a novel, profile-scale perspective on SOC drivers in a complex mountain region, presents a replicable framework for similar ecosystems, and supplies targeted data to guide soil carbon management and conservation strategies in the DMA.

2. Data and Methods

2.1. Study Area

The DMA is situated in central China (112°30'–117°10'E, 30°10'–32°30'N), at a pivotal ecological transition zone spanning parts of Hubei, Henan, and Anhui provinces (Figure 1). This study encompasses 61 county-level administrative units within this region. The DMA presents a highly suitable natural experimental system for studying the drivers of SOC across a full soil profile for several theoretical and practical reasons. Its core characteristic is pronounced environmental heterogeneity stemming from complex fault-block mountain terrain and hilly topography (>50% of the area). This terrain creates steep, covarying gradients in key state factors over short distances, including elevation (from near sea level to >1700 m), microclimate, soil moisture regimes, and vegetation types [29, 31, 32]. Such a configuration encapsulates a wide spectrum of conditions known to influence SOC dynamics, making it an ideal model for discerning the relative importance of different drivers.

Crucially, this region is particularly suited for investigating depth-dependent controls. First, under its humid subtropical monsoon climate (mean annual temperature of approximately 12.5 °C and precipitation of approximately 1832.8 mm), intense weathering has formed deep soil profiles, predominantly consisting of Haplic Luvisols and Ferralic Cambisols (classified locally as Yellow-Brown and Yellow Cinnamon soils) [31, 33, 34]. These profiles facilitate the examination of the theoretical transition in SOC governing mechanisms from biologically-driven, labile carbon cycling in surface horizons (0-30 cm) to geochemically-controlled, mineral-associated stabilization in the subsoil (>30 cm). Second, the landscape is a mosaic of natural forests, plantations, tea gardens, and terraced farmlands [35-37]. This

variety imposes distinct aboveground carbon input quantities and qualities, as well as management-driven disturbance regimes (e.g., tillage, fertilization), whose influences are known to attenuate differentially with depth. Studying the DMA therefore allows us to test how the influence of interactive controls like land use interacts with state factors like topography and parent material across the soil continuum, addressing a key gap in landscape-scale SOC studies.

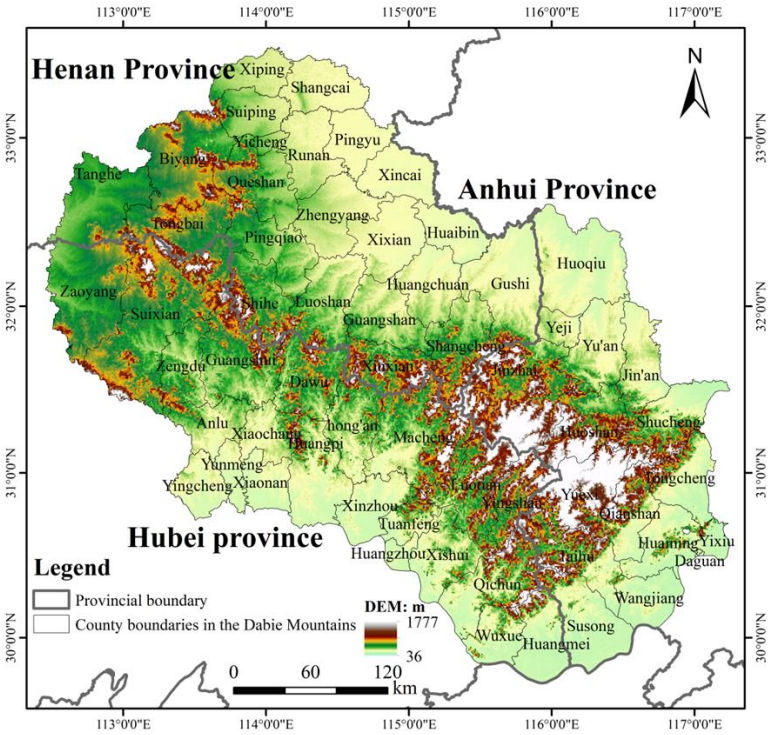

Figure 1. Location map of the study area

2.2. Data Sources and Preprocessing

This study integrated multi-source spatial data primarily from the year 2017 to build a comprehensive geodatabase (Table 1). The core dataset comprised high-resolution (250 m) gridded measurements of SOC content and key soil physicochemical properties (pH, particle size distribution, bulk density, etc.), stratified across six depth intervals [38]. Complementary data included a 30 m resolution digital elevation model (DEM) and its derivatives (e.g., slope and aspect), 1 km resolution climatic data (mean annual temperature and precipitation), soil type maps, and a 10 m resolution land cover classification [39].

To ensure spatial consistency for integrated analysis, all raster datasets were reprojected to an Albers equal-area conic projection (based on the WGS84 datum) and resampled to a unified 1 km spatial resolution using a bilinear algorithm for continuous variables and a majority filter for categorical data. This resolution was chosen as a pragmatic scale for regional analysis, effectively capturing major environmental gradients while being consistent with the scale of climate data and reducing the computational burden of spatial statistical operations.

Table 1. Data sources used in the study

Data	Time	Data Type	Data Source
SOC content	2017	Raster (250 m)	National Earth System Science Data Center (http://www.geodata.cn/)
Elevation (X1)	—	Raster (30 m)	Resource and Environment Science and Data Center (https://www.resdc.cn/)
Slope (X2)	—	Raster (30 m)	Resource and Environment Science and Data Center (https://www.resdc.cn/)
Aspect (X3)	—	Raster (30 m)	Resource and Environment Science and Data Center (https://www.resdc.cn/)
Temperature (X4)	2017	Raster (1 km)	Resource and Environment Science and Data Center (https://www.resdc.cn/)
Precipitation (X5)	2017	Raster (1 km)	Resource and Environment Science and Data Center (https://www.resdc.cn/)
Soil type (X6)	2017	Raster (1 km)	Resource and Environment Science and Data Center (https://www.resdc.cn/)
Land cover (X7)	2017	Raster (10 m)	Esri Land Cover (https://livingatlas.arcgis.com/landcover/)
Soil pH (X8)	2017	Raster (250 m)	National Earth System Science Data Center (http://www.geodata.cn/)
Soil Sand Content (SSC) (X9)	2017	Raster (250 m)	National Earth System Science Data Center (http://www.geodata.cn/)
Soil Clay Content (SCC) (X10)	2017	Raster (250 m)	National Earth System Science Data Center (http://www.geodata.cn/)
Soil Bulk Density (SBD) (X11)	2017	Raster (250 m)	National Earth System Science Data Center (http://www.geodata.cn/)
Soil Silt Content (SiC) (X12)	2017	Raster (250 m)	National Earth System Science Data Center (http://www.geodata.cn/)
Soil Gravel Volume Fraction (SGVF) (X13)	2017	Raster (250 m)	National Earth System Science Data Center (http://www.geodata.cn/)
Soil Cation Exchange Capacity (SCEC) (X14)	2017	Raster (250 m)	National Earth System Science Data Center (http://www.geodata.cn/)

2.3. Methodological Framework

2.3.1. Hot Spot Analysis (*Getis-Ord Gi**)

To identify statistically significant spatial clusters of high and low SOC values (hot spots and cold spots) at each depth interval, we employed the *Getis-Ord Gi** statistic, a local indicator of spatial association (LISA) [40]. This method calculates a Z-score for each grid cell, indicating whether high or low values cluster spatially around it [41]. The statistic is defined as:

$$G_i^* = \frac{\sum_{j=1}^{n} wij(d)x_j - \bar{X}\sum_{j=1}^{n} wij(d)}{S\sqrt{\frac{n\sum_{j=1}^{n} w_{ij}^2(d) - \left[\sum_{j=1}^{n} wij(d)\right]^2}{n-1}}} \quad (1)$$

where, x_j is the SOC value at location j, $wij(d)$ is a spatial weight matrix defining neighborhood relationships within a distance threshold d, n is the total number of locations, $\bar{X}$ is the mean SOC, and S is the standard deviation. A fixed-distance neighborhood was determined through incremental spatial autocorrelation analysis.

Based on the *Getis-Ord Gi** results, areas were reclassified into five categories: statistically significant cold spots (99% confidence) and hot spots (99% confidence), sub-cold spots and sub-hot spots (95% or 90% confidence), and areas with no statistical significance.

2.3.2. Geographical Detector Model

To quantitatively assess the individual and combined influences of potential drivers on SOC spatial heterogeneity, we used the Geographical Detector model [42]. This method is particularly adept at detecting spatial stratified heterogeneity and factor interactions without requiring linear assumptions [43, 44].

The model is grounded in the principle that if an independent variable (X) strongly influences a dependent variable (Y), their spatial distributions will exhibit similarity [43]. This relationship is quantified via the factor detector using a q-statistic [43]:

$$q = 1 - \frac{\sum_{□=1}^{L} N_□ \sigma_□^2}{N\sigma^2} \quad (2)$$

where, h=1, ..., L represents strata of variable X; N_h and N are the number of observations in stratum $h$and the overall region, respectively; σ_h^2 and σ^2 are the variances of Y within stratum h and the entire region. The value q ($0 \leq q \leq 1$) denotes the proportion of Y's spatial variance explained by X, with higher values indicating greater explanatory power. The model assumes spatial stratified heterogeneity (SSH), meaning the study area can be partitioned into strata where within-stratum variance of Y is minimized. This assumption was considered inherently valid for our explanatory variables in the topographically and climatically complex DMA.

The interaction detector module of the geographical detector was employed to quantify how pairs of influencing factors interactively enhanced or weakened their combined explanatory power over SOC spatial heterogeneity, with the resulting interaction types (e.g., nonlinear enhancement) helped elucidate the underlying coupled ecological and pedological processes [45]. The factors considered, including elevation (X1), slope (X2), aspect (X3), temperature (X4), precipitation (X5), soil type (X6), land cover (X7), soil pH (X8), Soil Sand Content (SSC) (X9), Soil Clay Content (SCC) (X10), Soil Bulk Density (SBD) (X11), Soil Silt Content (SiC) (X12), Soil Gravel Volume Fraction (SGVF) (X13), and Soil Cation Exchange Capacity (SCEC) (X14), are presented in Table 1.

In terms of variable processing, continuous variables (e.g., elevation, soil properties) were discretized into strata using the Jenks natural breaks classification method, which maximizes variance between classes. Categorical variables (land cover, soil type) were used in their native classes [46]. We acknowledge intercorrelations among some soil properties (e.g., texture fractions, bulk density). The Geographical Detector addresses the issue of collinearity differently from conventional regression models, primarily due to its methodological foundations: (1) The q-statistic quantifies how well a factor's spatial stratification explains the spatial pattern of SOC, rather than estimating its independent partial effect within a linear equation. This variance-based approach inherently reduces sensitivity to traditional multicollinearity [43]. (2) The interaction detector can effectively reveal whether the combined influence of two factors is nonlinearly enhanced, independent, or weakened. This allows for the examination of synergistic effects even between correlated variables [47]. As a supplementary measure, we calculated Variance Inflation Factors (VIFs) for all continuous variables, which were consistently below 5, further confirming that collinearity does not critically undermine the interpretability of our inputs [48].

2.3.3. Methodological Workflow

To clearly illustrate the analytical process of this study, a comprehensive workflow chart is presented in Figure 2. The methodology encompassed three major phases: (1) Data Preparation, involving the collection of multi-source spatial data (SOC content, topography, climate, soil properties, and land cover), followed by coordinate unification, resampling,

and variable discretization to construct an integrated geodatabase; (2) Spatial Pattern and Driver Analysis, which applied Hot Spot Analysis (*Getis-Ord Gi**) to identify significant spatial clusters (hot/cold spots) of SOC at each depth interval, and employed the Geographical Detector model (including Factor and Interaction Detector modules) to quantify the individual and interactive influences of environmental factors on SOC heterogeneity; (3) Synthesis and Interpretation, where the results from both spatial and statistical analyses were integrated to elucidate the vertical zonation of SOC distribution and the depth-dependent shifts in its dominant controlling mechanisms.

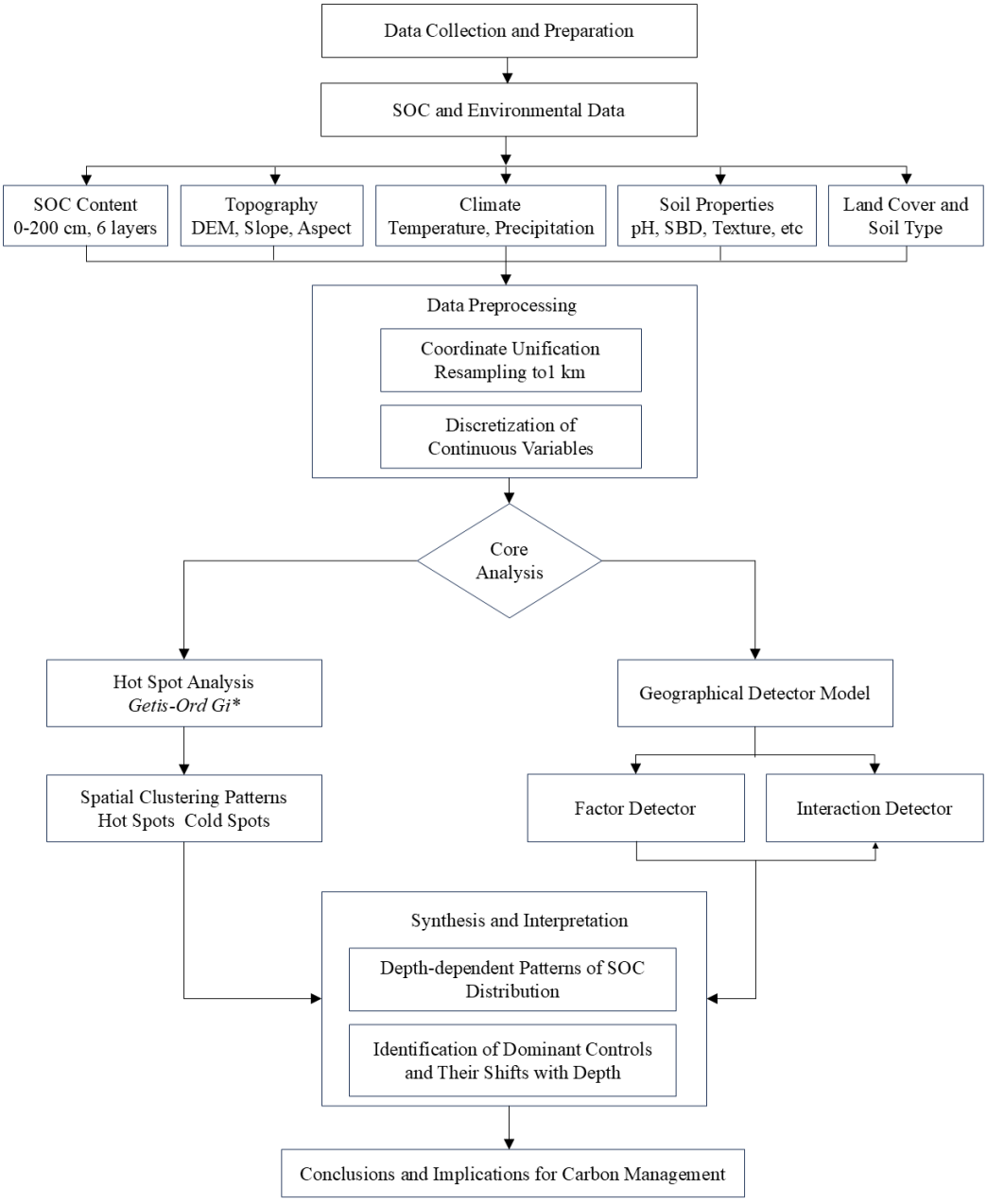

Figure 2. Methodological workflow of the study

2.4. Considerations of Data and Methodological Choices

Concerning the temporal scope of our data, the analysis is based on a 2017 snapshot. While interannual climate variability can affect labile SOC pools, the spatial distribution of total SOC stock is largely shaped by long-term averages of climate, persistent soil properties, and stable land use patterns. The identified spatial relationships are thus considered robust for understanding dominant controls, though this design precludes analysis of temporal trends—a recognized limitation for future work with time-series data [15].

Regarding the spatial scale of analysis, resampling high-resolution data (e.g., 10 m land cover) to 1 km inevitably smooths fine-scale heterogeneity. However, 1 km was selected as a standard and appropriate scale for regional SOC driver analysis, as it captures the major environmental gradients controlling SOC at this extent while enabling integration of key climatic datasets [49]. Interpretations are framed within this regional context.

Concerning the depth stratification, the six depth intervals correspond to standard pedogenic and functional zones: 0-5 cm (surficial, high biological activity), 5-15 cm (upper root zone), 15-30 cm (lower topsoil/plow layer), 30-60 cm (illuvial B horizon, transition zone), 60-100 cm and 100-200 cm (deeper subsoil and saprolite, dominated by older, mineral-associated carbon) [50]. This stratification allows explicit testing for shifts in driver importance across these functionally distinct layers.

3. Results

3.1. Spatial Distribution Characteristics of SOC Content

3.1.1. Spatial Pattern and Vertical Zonation

Following the classification standard of Li et al. [51], the SOC content in the DMA was classified into six grades, as shown in Figure 3. The spatial distribution of SOC across the six investigated depth intervals revealed a clear and consistent vertical zonation pattern within the DMA. As anticipated, SOC content exhibited a marked exponential decline with increasing soil depth. The surface layer (0–5 cm) harbored the highest concentrations, with a mean of 27.14 g/kg and a substantial proportion of the area (46.25%) exceeding 24 g/kg. This contrasted sharply with the deepest layer (100–200 cm), where the mean SOC content was only 3.84 g/kg and 77.04% of the area fell within the 3–6 g/kg range. This vertical pattern aligns with the global paradigm in which SOC is primarily concentrated in surface horizons due to direct litterfall inputs, rhizodeposition, and limited translocation depth [52-54].

Spatially, a distinct core-periphery structure (characterized by higher SOC in central areas and lower SOC in peripheral zones) was evident, particularly in the upper 30 cm, with high SOC in the central region and lower SOC in the surrounding areas. This core area of elevated SOC corresponded geographically to the contiguous, high-elevation forested regions of Yuexi, Huoshan, Jinzhai, and Yingshan counties. In contrast, the peripheral low-SOC belt, including areas like Queshan and Huangchuan, predominantly consisted of lower-relief terrain under intensive agriculture. This pattern suggests a strong coupling between SOC, topography (which controls microclimate and vegetation), and land use; a relationship commonly observed in mountainous regions worldwide (e.g., the European Alps [55], and the Himalayan region [56]). A critical transition occurred below approximately 60 cm. The sharp spatial contrasts characteristic of the surface layers were significantly attenuated, giving way to a more spatially homogeneous and evenly distributed pattern with weaker geographical structuring (Figure 3d-f). This suggests that the drivers creating strong spatial autocorrelation at the surface lose their influence with depth, pointing to a shift in governing processes for subsoil carbon [53, 54].

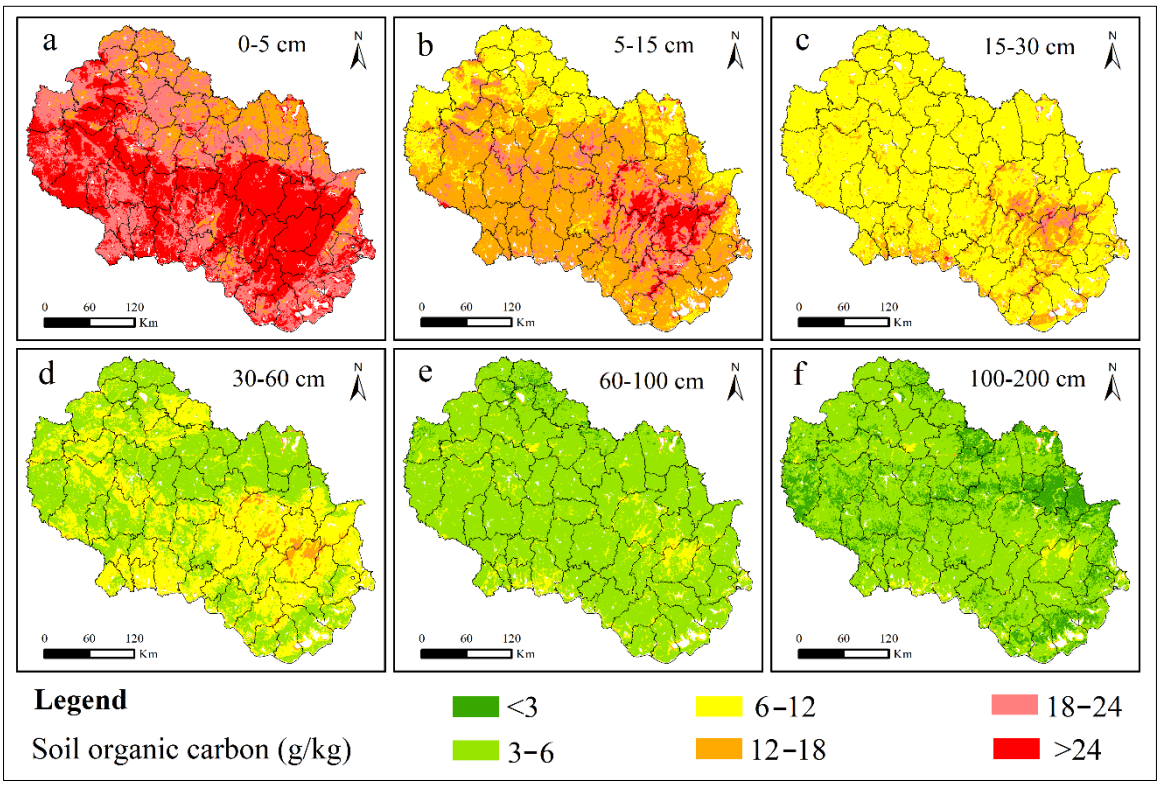

Figure 3. Spatial distribution of SOC content at different depths in DMA. (a) 0-5 cm, (b) 5-15 cm, (c) 15-30 cm, (d) 30-60 cm, (e) 60-100 cm, and (f) 100-200 cm

3.1.2. Statistical Summary and Depth-Wise Variability

Descriptive statistics further quantified these patterns (Table 2). The mean SOC content decreased by over 85% from the surface (0–5 cm) to the deepest layer (100–200 cm), consistent with the global vertical attenuation pattern of SOC [52]. Notably, the surface layer not only had the highest mean but also the greatest absolute variability (SD = 10.44 g/kg) and range (77.90 g/kg). This high surface variability reflects the acute sensitivity of topsoil SOC to the heterogeneous interplay of local environmental factors such as vegetation type, land management, and microtopography [15]. The Coefficient of Variation (CV) across all layers ranged from 25.7% to 38.5%, indicating a moderate level of spatial variability according to the classification by Nielsen & Bouma [57]. Importantly, the distribution of SOC values was strongly right-skewed with high kurtosis (leptokurtic) for all layers below 5 cm. This statistical profile indicates that the majority of the landscape is characterized by moderate to low SOC values, while a smaller proportion of the area—the identified "hot spots"—contains very high values, elevating the mean. This is a common feature in soil property distributions [58] and underscores the importance of identifying and understanding these high-value clusters.

Table 2. Descriptive statistics of soil organic carbon (SOC) content at different soil depths

Soil depth (cm)	SOC content/(g/kg)			Stand. Dev.	Coefficient of variation (%)	Skewness	Kurtosis
	Minimum	Mean	Maximum				
0-5	8.60	27.14	86.50	10.44	38.47	1.30	1.29
5-15	5.90	15.34	60.80	5.30	34.55	1.94	6.06
15-30	5.30	10.08	39.10	2.59	25.69	2.04	6.64
30-60	1.90	6.69	30.50	2.21	33.03	1.90	5.22
60-100	1.60	4.69	28.70	1.32	28.14	3.03	17.59
100-200	0.90	3.84	29.00	1.25	32.55	3.89	25.43

3.2. Evolution of Spatial Clustering with Depth: Insights from Hot Spot Analysis

The *Getis-Ord Gi** analysis revealed a quantitative and nuanced view of how the spatial organization of SOC changes with depth (Figure 4). In the topsoil (0–5 cm), SOC exhibited pronounced and statistically significant spatial clustering. Well-defined hot spots (25.4% of the area) are concentrated in the central forested highlands, while extensive cold spots (59.6%) dominate the peripheral agricultural lowlands. This pattern confirmed the strong, localized control of surface drivers like land cover and topographic position.

A profound transformation in this spatial structure occurred with increasing depth. The areal extent of significant hot spots contracted dramatically, from 26.6% at 5–15 cm to merely 8.7% at 100–200 cm. More telling than the mere reduction in area is the dispersion and fragmentation of these clusters. Below the 60 cm threshold, the previously cohesive hot spot region in the central mountains fragmented, with clusters becoming more scattered, particularly towards the southern margins of the DMA. Concurrently, the proportion of area classified as "insignificant" (showing no clear clustering) increased from 9.1% at the surface to 41.9% in the deepest layer.

This spatial reorganization indicates a clear shift in the dominant controls governing SOC distribution with depth. Specifically, the transition from strong, coherent clustering in shallower layers to a weak, dispersed pattern below approximately 60 cm is mechanistically important and supports evolving conceptual models in soil carbon science. In surface soils, SOC distribution is tightly coupled to spatially discrete and heterogeneous "first-order" controls. These include vegetation community composition (e.g., forest vs. cropland), land-use practices (tillage, fertilization), the quantity and quality of fresh litter inputs, and fine-scale topographic effects on soil moisture and temperature. These factors create sharp local gradients, which leads to strong positive spatial autocorrelation (clustering) [53].

In contrast, subsoil SOC (>60 cm) consists largely of older, more processed carbon that has undergone translocation (e.g., via leaching, bioturbation) and long-term stabilization, often through association with mineral surfaces [54, 59]. Its distribution becomes increasingly decoupled from these immediate surface controls. Instead, it is governed by factors that operate over broader spatial scales or exhibit less patchiness: the geochemical and mineralogical composition of the parent material, which varies more gradually across landscapes; regional groundwater dynamics influencing leaching and redox conditions; historical pedoturbation processes (e.g., clay illuviation, weathering); and long-term organo-mineral interaction potentials [53]. These subsoil processes often have a spatially homogenizing effect, smoothing out the sharp contrasts imposed by surface heterogeneity. Consequently, the strong spatial signature imprinted at the surface fades, leading to the observed dispersion and eventual dominance of "insignificant" spatial patterns. This supports the conceptual model of a depth-dependent shift from a biologically dominated surface regime (where inputs and rapid cycling create spatial hot spots) to a geochemically dominated subsoil regime (where slower stabilization and parent material legacy promote spatial homogenization) [54].

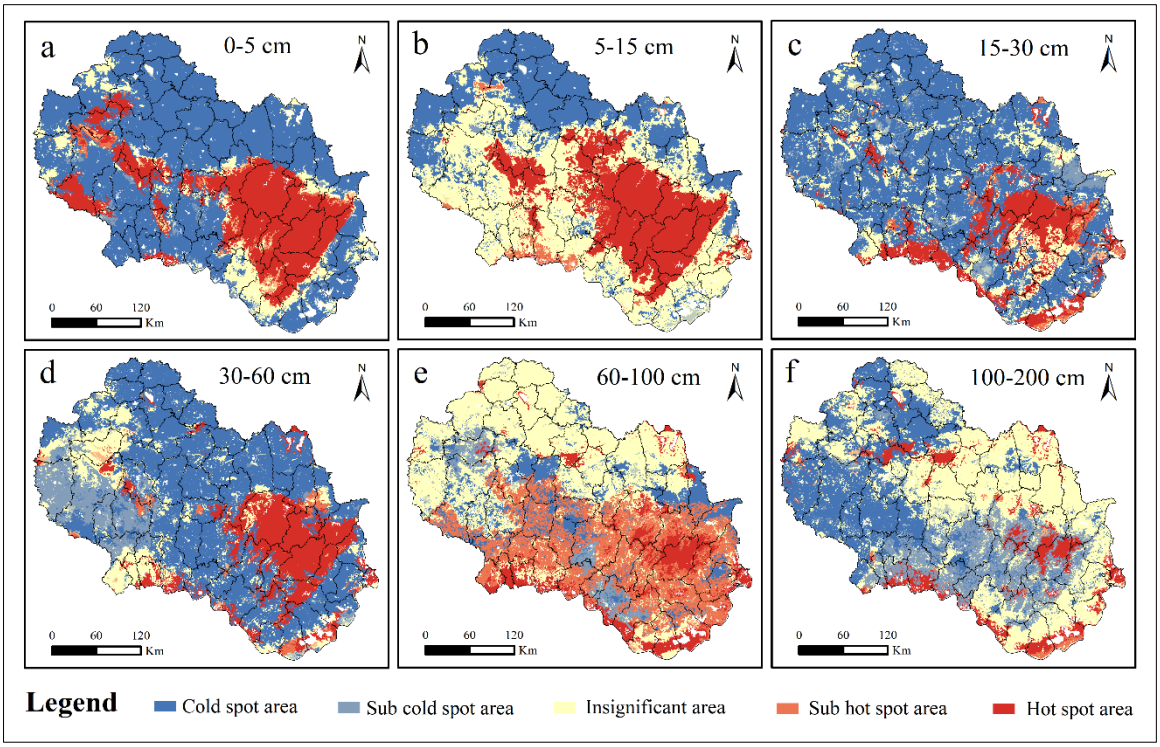

Figure 4. Spatial distribution of cold spot and hot spot areas of SOC content at different soil depths in the DMA. (a) 0-5 cm, (b) 5-15 cm, (c) 15-30 cm, (d) 30-60 cm, (e) 60-100 cm, and (f) 100-200 cm

3.3. Dominant Controls on SOC Heterogeneity: A Depth-Resolved Perspective

3.3.1. Factor Detection: Shifting Hierarchies of Influence

The geographical detector's factor analysis (q-statistic) quantified the individual explanatory power of 14 potential drivers (Figure 5). Averaged across all depths, elevation (q=0.403) and SBD (q=0.401) emerged as the two most influential factors, underscoring the paramount role of topography (as an integrative proxy for climate and vegetation) and soil physical structure (controlling porosity and protection) in the DMA. Temperature (q=0.344) and soil pH (q=0.332) were the next most important, while factors like aspect and soil type showed minimal explanatory power.

A critical insight from this analysis is the depth-dependent shift in the hierarchy of controlling factors. In the surface layers (0–15 cm), spatial heterogeneity was predominantly governed by the interplay of topography (elevation) and key edaphic properties (soil pH and SBD). The dominance of elevation reflects its master control over temperature, precipitation, and the resultant vegetation productivity that governs carbon inputs. The concurrent strong influence of pH and SBD highlights that the initial stabilization of this fresh carbon is highly sensitive to the local chemical environment (governing microbial activity and organo-mineral complexation) and physical protection mechanisms (aggregation, occlusion).

Moving to the subsurface layers (15–200 cm), the explanatory dynamics shifted. The relative importance of direct climatic factors (temperature and precipitation) increased significantly, rivaling or surpassing that of elevation in the deeper horizons. While SBD remained a consistently influential soil property, this pattern suggests a conceptual transition: whereas topography sets the initial template for carbon input at the surface, the fate of carbon that is translocated to or persists in the subsoil becomes increasingly governed by regional climate conditions. These conditions affect temperature-sensitive mineralization kinetics and moisture-driven dissolution and translocation processes, all interacting with the persistent, depth-independent soil property of bulk density.

Furthermore, the explanatory power (q-value) of most factors diminished with depth. Elevation and soil pH exhibited the largest absolute declines. Notably, the influence of SCEC and SGVF nearly vanished (decreasing by >95%), indicating that their relevance is largely confined to the more dynamic, chemistry-driven surface environment rather than the aged, mineral-stabilized subsoil carbon pool.

These findings can be contextualized within the global understanding of SOC drivers. The primacy of elevation in governing SOC patterns in mountainous regions is a consistent finding, aligning with research in the Alps, Andes, and Himalayas, where it integrates fundamental energy and moisture gradients [55, 60]. The persistent, strong effect of SBD supports global syntheses that identify physical protection as a critical, depth-independent stabilization mechanism [59].

The increasing relative role of direct climatic variables with depth presents a more nuanced insight. It contrasts with some studies that report an attenuation of climate signals with depth [52] but corroborates others, particularly in humid regions like the DMA, where hydro-climatic drivers strongly influence deep carbon dynamics via leaching and moisture-regulated processes [54]. This divergence underscores the context-specificity of deep SOC controls, which are likely modulated by regional climate regime, drainage conditions, and soil mineralogy.

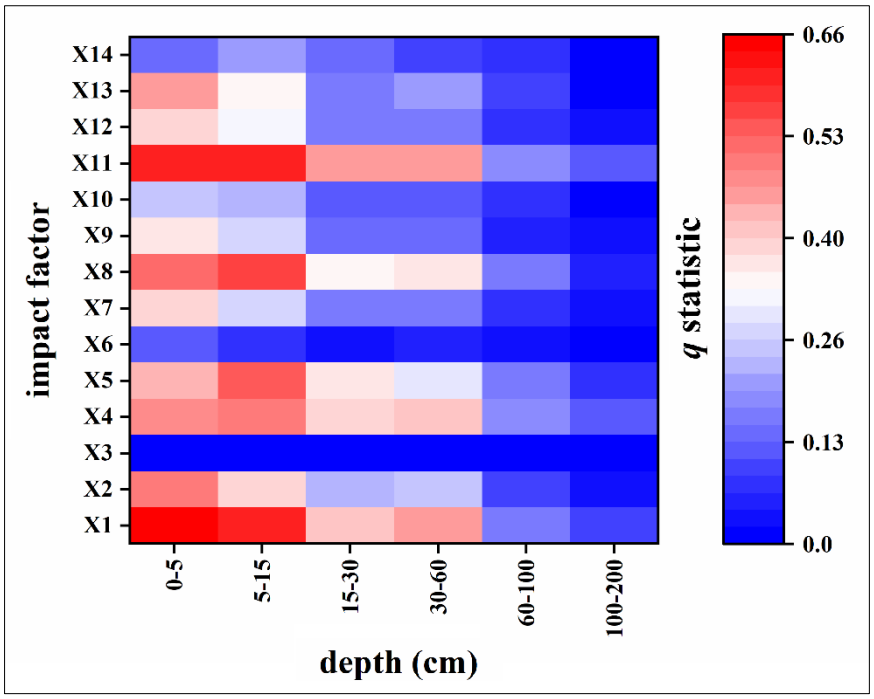

Figure 5. The *q* statistic for factor detection results of SOC content in DMA

3.3.2. Interaction Detection Results of SOC Content

The interaction detector revealed that combined factor effects always surpassed individual ones, demonstrating nonlinear enhancement (Figure 6). This underscores that SOC distribution is not governed by simple additive effects but by complex interdependencies [47]. On average, the most powerful synergistic interactions were between temperature ∩ soil pH (q=0.479) and temperature ∩ precipitation (q=0.473), highlighting the fundamental role of climate-soil interactions across the entire profile.

A depth-specific analysis, however, reveals a pivotal transition in the dominant interactive mechanisms. In the surface soils (0–15 cm), the strongest interactions involved elevation ∩ SBD and elevation ∩ soil pH. This indicates that the effect of topography on SOC is significantly modulated by local soil conditions [60]. For instance, at a given elevation (and thus under a similar climatic and vegetative regime), soils with higher bulk density (which can restrict decomposition and oxygen diffusion) or a more acidic pH (which can inhibit specific microbial activities) can lead to enhanced SOC sequestration.

At greater depths (15–200 cm), the dominant interactions shifted decisively to temperature ∩ soil pH and temperature ∩ precipitation. This suggests that in deeper layers, where direct carbon inputs are minimal, the influence of climate on processes such as chemical weathering, dissolved organic carbon transport, and long-term decomposition rates is strongly contingent upon the soil's chemical environment (pH) [54] and its moisture regime (influenced by precipitation). The pronounced synergy between temperature and precipitation is particularly telling, pointing to the critical importance of coupled hydro-thermal regimes in controlling the persistence and turnover of subsoil carbon.

Taken together, these results articulate a coherent, depth-resolved framework for SOC governance in the DMA. The spatial heterogeneity of surface SOC is sculpted primarily by the interactive template of topography and immediate soil properties, which co-determine carbon input regimes and early stabilization pathways. In contrast, the spatial pattern of deep SOC is increasingly a legacy of the interaction between regional climate and subsoil geochemistry, which jointly control the long-term stabilization and storage of carbon that has escaped rapid surface cycling. This represents a conceptual shift from a topo-edaphic dominated surface regime to a climate-edaphic dominated subsoil regime [53]. Our findings resonate with the growing body of literature emphasizing the changing nature of SOC controls with depth but provide a quantified, mechanistic insight into the specific factor interactions driving this shift in a subtropical montane ecosystem.

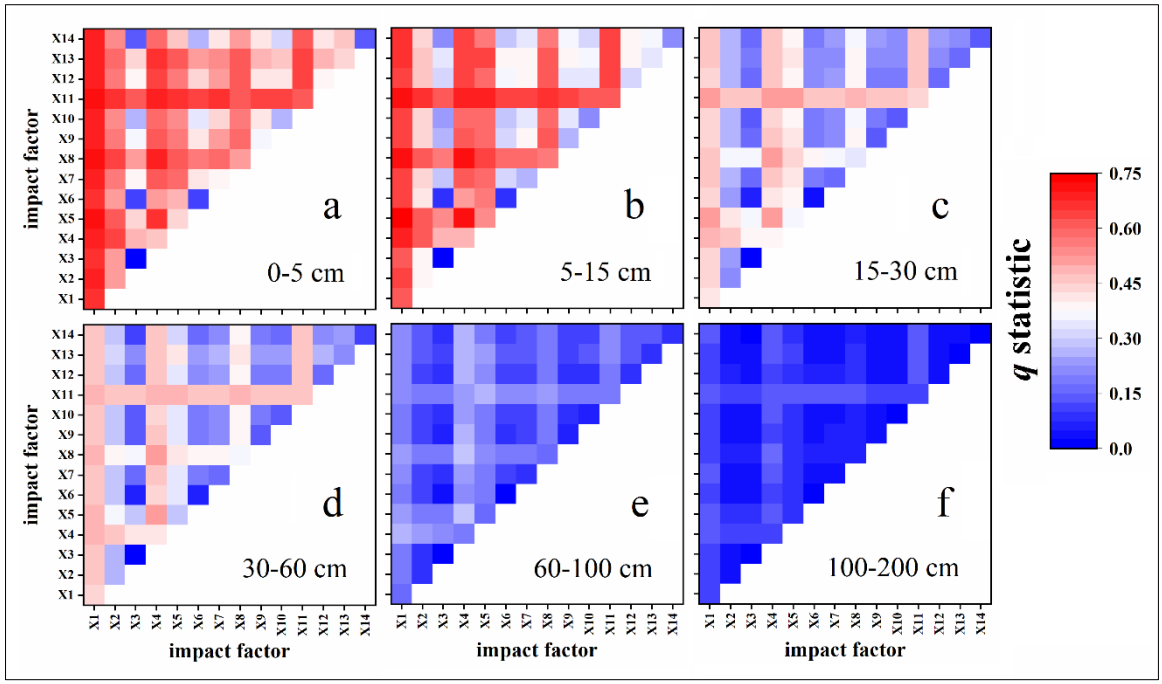

Figure 6. The *q* statistics for the interaction detection results of SOC content in DMA. (a) 0-5 cm, (b) 5-15 cm, (c) 15-30 cm, (d) 30-60 cm, (e) 60-100 cm, and (f) 100-200 cm

4. Discussion

This study reveals that SOC content in the DMA follows a pronounced vertical distribution pattern, characterized by an exponential decrease with increasing soil depth and significant surface aggregation within the top 0–10 cm. This pattern aligns with findings from diverse regions, such as the Guanzhong Plain [61] and the Cangshan Mountains [62], and confirms its prevalence across varied ecosystems. The underlying mechanism is well-established: surface litter serves as the primary source of soil organic matter, while deeper soils are more stable and experience limited fresh input and disturbance, leading to a concentration of SOC in surface layers, while translocation results in the characteristic top-down decline [54, 59]. Previous research has further demonstrated that SOC storage varies significantly among distinct ecosystems [52], and within any given ecosystem, SOC is primarily concentrated in the surface layer [63], with significant differences emerging in its vertical distribution as depth increases [54, 64]. For instance, in karst regions of southern China, forested areas were found to have higher SOC content in the 0-50 cm layer compared to wastelands, gardens, orchards, grasslands, and farmlands [65]. Similarly, on the Loess Plateau, SOC content and its influencing factors showed significant correlations with depth across a 0-180 cm profile [66].

As shown in Figure 7, the ranking of SOC content among four typical terrestrial ecosystems (forest, grassland, wetland, cropland) varies with depth, highlighting the dynamic interplay between carbon input and stabilization processes. The SOC content in surface soil (0–15 cm) and at 30–60 cm depth follows the order: forest > grassland > wetland > cropland. At depths of 15–30 cm and 60–100 cm, the order shifts to wetland > forest > grassland > cropland. In the deepest layer (100–200 cm), the order becomes wetland > grassland > forest > cropland. This variation underscores the significant impact of soil depth on SOC content across terrestrial ecosystems. Among these, the forest ecosystem exhibits the most dramatic decline, with SOC content dropping from 38.16 g/kg at 0–5 cm to 3.99 g/kg at 100–200 cm. Conversely, the wetland ecosystem experiences the smallest decline, retaining 81.28% of its SOC content from the surface to the deepest layer. The presence of trees, shrubs, and a thick litter layer in forests provides substantial carbon input, making forestland the land use with the highest average SOC content (14.47 g/kg in the 0-200 cm profile) [67]. Grasslands, with diverse plant litter and root exudates, also facilitate SOC accumulation [68]. The SOC in wetlands exceeds that in croplands, which is attributed to the warm DMA climate favoring decomposition and humus formation over peat accumulation [69]. In contrast, cropland, most influenced by human activity through harvest removal and tillage, exhibits the lowest SOC levels due to minimized organic matter return and accelerated decomposition [70, 71].

The study identified elevation and its interaction with soil pH and SBD as the primary factors influencing the spatial distribution of SOC in the topsoil layer (0-15 cm) of the DMA (Figures 5 & 6). This aligns with the findings from Mount Bambouto [72] and Yunnan Province [73] but contrasts with studies in the Colombian [74] and Peruvian Andes [75] where SOC showed no significant altitudinal trend. Elevation integrates gradients of water, heat, and light, which directly and indirectly influence SOC by affecting plant biomass, soil properties, and microbial activity [76-78]. Soil pH serves

as a key determinant, potentially mitigating decomposition by shaping microbial community structure [79]. SBD impacts soil permeability, water retention, and vegetation growth, thereby regulating organic matter input and accumulation [80].

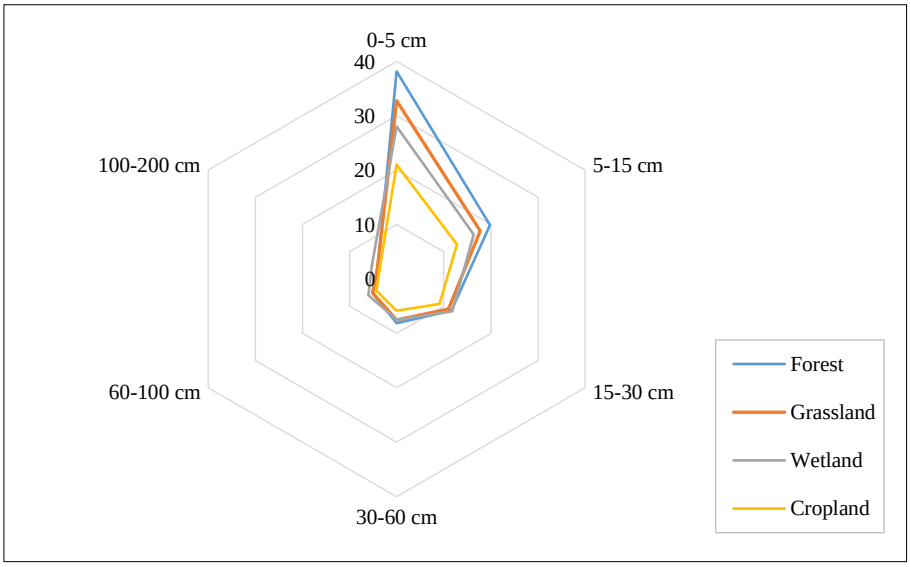

Figure 7. SOC content across different soil depths in four terrestrial ecosystems within the DMA

Climate factors significantly impact both the input and decomposition of SOC. Vegetation productivity driven by climate controls carbon input, while microbial activity regulated by soil moisture and temperature controls its decomposition and turnover [81, 82]. Increases in temperature and precipitation can enhance photosynthesis and carbon input but may also elevate respiration and decomposition rates, leading to potential SOC loss [82, 83]. The spatial distribution of SOC in deeper layers (15–200 cm) is mainly influenced by meteorological factors and their interaction with soil pH and SBD, a finding consistent with research in dryland farming regions of China [84] and at a global scale [85]. This indicates that hydrothermal factors are crucial in governing SOC variation characteristics in subsoils.

5. Conclusion

This study has delivered a comprehensive, depth-resolved analysis of the spatial patterns and driving mechanisms of SOC throughout the 0–200 cm profile in the DMA, a subtropical montane ecosystem of central China. Through the integration of high-resolution SOC data with a comprehensive set of environmental variables and the application of spatial statistics (*Getis-Ord Gi**) and the geographical detector model, we progressed beyond a surface-centric view to establish a three-dimensional understanding of SOC storage and its controls. The key conclusions are outlined below:

First, our results confirm a sharp exponential decline in SOC content with depth, with the surface 0–5 cm layer storing approximately 40% of the total profile SOC stock. More importantly, we identified a fundamental shift in the spatial organization of SOC at approximately 60 cm depth. Surface layers (0–60 cm) exhibited strong, spatially coherent clustering (distinct hot spots and cold spots), which transitioned to a significantly weaker, more dispersed, and fragmented pattern in the subsoil (>60 cm). This spatial reorganization is interpreted as a transition from a biologically dominated surface regime—where carbon distribution is tightly coupled to clustered patterns of vegetation, land use, and micro-topography governing input and early decomposition—to a geochemically dominated subsoil regime. At greater depths, SOC consists of older, mineral-associated or mineral-stabilized organic matter whose distribution is increasingly decoupled from immediate surface processes and is instead shaped by the more gradual, spatially complex heterogeneity of parent material mineralogy, historical pedogenesis (e.g., illuviation), and long-term organo-mineral interactions, leading to spatial homogenization.

Second, the geographical detector analysis yielded a quantitative measure of a clear depth-dependent hierarchy in the individual and interactive controls on SOC heterogeneity. Elevation and SBD were the two most influential factors on average across the profile, affirming the overarching roles of topography (which integrates climate and vegetation) and soil physical protection. Nonetheless, their relative importance and interactions changed notably with depth. In surface soils (0–15 cm), SOC variability was predominantly explained by the synergistic interactions between topography (elevation) and edaphic properties (pH, SBD), forming a topo-edaphic control complex. In contrast, within the subsoil (15–200 cm), the dominant interactions shifted to those between regional climate (temperature, precipitation) and soil properties (pH, SBD), defining a climate-edaphic control complex. This shift signifies that while topography sets the template for surface carbon inputs, the fate of deep, legacy carbon is governed by the interplay of regional climatic conditions (affecting long-term decomposition and translocation kinetics) and subsoil geochemistry.

In summary, this research articulates a coherent vertical paradigm for SOC governance in the DMA, demonstrating that the factors controlling SOC are not static but transition with depth in both their spatial expression and their

interactive dominance. These findings bridge a critical knowledge gap by providing a quantified, mechanistic framework that explains why surface SOC maps show high spatial predictability while subsoil carbon distributions appear more muted and complex. For ecosystem management, our work suggests that strategies to enhance surface SOC (e.g., afforestation, conservation tillage) must be location-specific, targeting areas where topography and soil conditions synergistically favor sequestration. Conversely, conserving the vast and stable subsoil carbon pool requires a focus on managing landscape-scale processes that affect hydro-thermal regimes and soil geochemical stability. This depth-resolved perspective offers a replicable analytical framework for other mountain ecosystems and provides a scientific basis for stratified carbon management strategies in the ecologically critical DMA. Future research should utilize process-based models informed by these documented interactions to evaluate the vulnerability of different carbon pools to climate and land use change.

6. Abbreviations

SOC	Soil Organic Carbon	DMA	Dabie Mountain Area
SBD	Soil Bulk Density	GD-SRK	Geographic Detector Based Hierarchical Regression Kriging
DEM	Digital Elevation Model	LISA	Local Indicator of Spatial Association
SSH	Spatial Stratified Heterogeneity	SSC	Soil Sand Content
SCC	Soil Clay Content	SiC	Soil Silt Content
SGVF	Soil Gravel Volume Fraction	SCEC	Soil Cation Exchange Capacity
VIFs	Variance Inflation Factors		

7. Declarations

7.1. Data Availability Statement

The data presented in this study are available on request from the corresponding author.

7.2. Funding

This research was supported by the Philosophy and Social Science Planning Project of Henan Province (Grant No. 2024CSH034), the Science and Technology Project of Henan Province (Grant No. 262400410008), the Natural Science Foundation of Henan Province (Grant No. 262300420637), and the Humanities and Social Sciences Research Projects of Henan Provincial Department of Education (Grant No. 2025-ZDJH-597).

7.3. Acknowledgments

Acknowledgement for the data support from “National Earth System Science Data Center, National Science & Technology Infrastructure of China (http://www.geodata.cn)”.

7.4. Institutional Review Board Statement

Not applicable.

7.5. Informed Consent Statement

Not applicable.

7.6. Declaration of Competing Interest

The author declares that they have no known competing financial interests or personal relationships that could have appeared to influence the work reported in this paper.

8. References

[1] Almendros, G., & González-Pérez, J. A. (2025). Soil Organic Carbon Sequestration Mechanisms and the Chemical Nature of Soil Organic Matter—A Review. Sustainability (Switzerland), 17(15), 6689. doi:10.3390/su17156689.

[2] Scharlemann, J. P. W., Tanner, E. V. J., Hiederer, R., & Kapos, V. (2014). Global soil carbon: Understanding and managing the largest terrestrial carbon pool. Carbon Management, 5(1), 81–91. doi:10.4155/cmt.13.77.

[3] Qing, Z., Liu, H., Meng, X., Du, B., Zhang, S., & Yu, M. (2025). Assessment of the synergistic effects of future climate change and land use on soil organic carbon stock in Northeast China. Catena, 260, 109456. doi:10.1016/j.catena.2025.109456.

[4] Hari, M., & Tyagi, B. (2022). Terrestrial carbon cycle: tipping edge of climate change between the atmosphere and biosphere ecosystems. Environmental Science: Atmospheres, 2(5), 867–890. doi:10.1039/d1ea00102g.

[5] Zhang, Y., An, C. B., Zhang, W. S., Zheng, L. Y., Zhang, Y. Z., Lu, C., & Liu, L. Y. (2023). Drivers of mountain soil organic carbon stock dynamics: A review. Journal of Soils and Sediments, 23(1), 64-76. doi:10.1007/s11368-022-03313-w.

[6] Zhang, L., Xu, T., Bai, Y., Wiesmeier, M., Li, H., Huang, Y., Liu, Y., Xie, B., Song, M., Wu, J., & Liu, C. (2025). Historical and future dynamics of soil organic carbon and driving mechanisms in mountainous soils of China. Catena, 258, 109212. doi:10.1016/j.catena.2025.109212.

[7] Li, S., Zhang, A., Song, H., Guo, W., Tang, Z., Lei, G., & Qi, L. (2023). The Dominant Factor Affecting Soil Organic Carbon in Subtropical Phyllostachys edulis Forests Is Climatic Factors Rather Than Soil Physicochemical Properties. Forests, 14(5), 958. doi:10.3390/f14050958.

[8] Blackburn, K. W., Libohova, Z., Adhikari, K., Kome, C., Maness, X., & Silman, M. R. (2022). Influence of Land Use and Topographic Factors on Soil Organic Carbon Stocks and Their Spatial and Vertical Distribution. Remote Sensing, 14(12), 2846. doi:10.3390/rs14122846.

[9] Wang, G., Li, J., Mao, J., Fan, L., Ma, X., Zhang, W., Liang, Y., Hui, T., & Li, Y. (2025). Multiscale drivers and tipping points regulating particulate and mineral-associated organic carbon across Central Asian grasslands. Geoderma, 464, 117610. doi:10.1016/j.geoderma.2025.117610.

[10] Bai, R., Zhao, X., Wang, X., Lv, W., Li, J., Yang, F., Shangguan, Z., & Deng, L. (2026). SOC erosion reduction of the "Grain for green" program on the Loess Plateau, China. Soil and Tillage Research, 256, 106863. doi:10.1016/j.still.2025.106863.

[11] Guo, B., Fang, M., Yang, L., Guo, T., Ma, C., Hu, X., Guo, Z., Ma, Z., Li, Q., Wang, Z., & Liu, W. (2026). Remapping carbon storage change in retired farmlands on the Loess Plateau in China from 2000–2021 in high spatiotemporal resolution. Earth System Science Data, 18(1), 429–441. doi:10.5194/essd-18-429-2026.

[12] Tiruneh, G. A., Righi, C. A., Polizel, J. L., Gonçalves, V., & Pereira, C. R. (2026). Modeling soil organic carbon in the Brazilian amazon with geostatistical and machine learning techniques. Trees, Forests and People, 23. doi:10.1016/j.tfp.2026.101150.

[13] Wan, Q., Zhu, G., Guo, H., Zhang, Y., Pan, H., Yong, L., & Ma, H. (2019). Influence of Vegetation Coverage and Climate Environment on Soil Organic Carbon in the Qilian Mountains. Scientific Reports, 9(1), 17623. doi:10.1038/s41598-019-53837-4.

[14] Mishra, U., & Riley, W. J. (2015). Scaling impacts on environmental controls and spatial heterogeneity of soil organic carbon stocks. Biogeosciences, 12(13), 3993–4004. doi:10.5194/bg-12-3993-2015.

[15] Wiesmeier, M., Urbanski, L., Hobley, E., Lang, B., von Lützow, M., Marin-Spiotta, E., van Wesemael, B., Rabot, E., Ließ, M., Garcia-Franco, N., Wollschläger, U., Vogel, H. J., & Kögel-Knabner, I. (2019). Soil organic carbon storage as a key function of soils - A review of drivers and indicators at various scales. Geoderma, 333, 149–162. doi:10.1016/j.geoderma.2018.07.026.

[16] Hobley, E., Wilson, B., Wilkie, A., Gray, J., & Koen, T. (2015). Drivers of soil organic carbon storage and vertical distribution in Eastern Australia. Plant and Soil, 390(1–2), 111–127. doi:10.1007/s11104-015-2380-1.

[17] Zhou, T., Lv, Y., Xie, B., Xu, L., Zhou, Y., Mei, T., Li, Y., Yuan, N., & Shi, Y. (2023). Topography and Soil Organic Carbon in Subtropical Forests of China. Forests, 14(5), 1023. doi:10.3390/f14051023.

[18] Kuśmierz, S., Skowrońska, M., Tkaczyk, P., Lipiński, W., & Mielniczuk, J. (2023). Soil Organic Carbon and Mineral Nitrogen Contents in Soils as Affected by Their pH, Texture and Fertilization. Agronomy, 13(1), 267. doi:10.3390/agronomy13010267.

[19] Liu, Y., Chen, Y., Wu, Z., Wang, B., & Wang, S. (2021). Geographical detector-based stratified regression kriging strategy for mapping soil organic carbon with high spatial heterogeneity. Catena, 196, 104953. doi:10.1016/j.catena.2020.104953.

[20] Liu, Z., Lei, H., Sheng, H., & Wang, Y. (2023). Analysis of soil organic matter influencing factors in the Huangshui River Basin by using the optimal parameter-based geographical detector model. Geocarto International, 38(1), 2246935. doi:10.1080/10106049.2023.2246935.

[21] Dubeux Jr, J. C., Lira Junior, M. D. A., Simili, F. F., Bretas, I. L., Trumpp, K. R., Bizzuti, B. E., Garcia, L., Oduor, K. T., Queiroz, L. M. D., Acuña, J. P., & Mendes, C. T. (2024). Deep soil organic carbon: A review. CABI Reviews, 2024(2), 1-17. doi:10.1079/cabireviews.2024.002.

[22] Zeng, X. M., Bastida, F., Plaza, C., Zhou, G., Vera, A., Liu, Y. R., & Delgado-Baquerizo, M. (2023). The Contribution of Biotic Factors in Explaining the Global Distribution of Inorganic Carbon in Surface Soils. Global Biogeochemical Cycles, 37(10), 7957. doi:10.1029/2023GB007957.

[23] Song, B., Wang, M., Zhang, S., Zhang, L., Lu, Y., Guo, H., Guo, X., Zhang, Y., & Zhou, X. (2025). Spatial distribution, drivers, and future variation of soil organic carbon in China's ecosystems: A meta-analysis and machine-learning assessment. Ecological Indicators, 179, 114255. doi:10.1016/j.ecolind.2025.114255.

[24] Ghosh, A., Singh, A. K., Kumar, S., Manna, M. C., Bhattacharyya, R., Agnihortri, R., Singh Gahlaud, S. K., Sannagoudar, M. S., Gautam, K., Kumar, R. V., & Chaudhari, S. K. (2020). Differentiating biological and chemical factors of top and deep soil carbon sequestration in semi-arid tropical Inceptisol: an outcome of structural equation modeling. Carbon Management, 11(5), 441–453. doi:10.1080/17583004.2020.1796143.

[25] Nie, X., Wang, D., Yang, L., & Zhou, G. (2021). Controls on variation of soil organic carbon concentration in the shrublands of the north-eastern Tibetan Plateau. European Journal of Soil Science, 72(4), 1817–1830. doi:10.1111/ejss.13084.

[26] Zhang, R., Liu, X., Heathman, G. C., Yao, X., Hu, X., & Zhang, G. (2013). Assessment of soil erosion sensitivity and analysis of sensitivity factors in the Tongbai-Dabie mountainous area of China. Catena, 101, 92–98. doi:10.1016/j.catena.2012.10.008.

[27] Yang, S. Y., Yang, K. F., Zhang, X. T., & Wang, J. (2011). The research of forest soil organic carbon accumulation in Dabie Mountain. Meteorological and Environmental Research, (3), 43-46. doi:CNKI:SUN:MEVR.0.2011-03-014.

[28] Qin, J., Liu, Y., Bi, Q., Chen, Z., & Zhang, B. (2023). Response of leaf and soil C, N and P stoichiometry in different Pinus massoniana forest types to slope aspect in the Dabie mountains region of North subtropical, China. Frontiers in Environmental Science, 11, 1148986. doi:10.3389/fenvs.2023.1148986.

[29] Fang, L., Liu, Y., Li, C., & Cai, J. (2023). Spatiotemporal Characteristics and Future Scenario Simulation of the Trade-offs and Synergies of Mountain Ecosystem Services: A Case Study of the Dabie Mountains Area, China. Chinese Geographical Science, 33(1), 144–160. doi:10.1007/s11769-023-1330-8.

[30] Dong, Q., Song, C., Wen, H., Xiang, J., Wang, P., & Yan, M. (2024). Comprehensive Geochemical Evaluation and Influencing Factors of Topsoil Nutrients in a Farming Area of Dabie Mountain in Western Anhui, China. Yankuang Ceshi, 43(2), 344–355. doi:10.15898/j.ykcs.202206180117.

[31] Zheng, L., Sun, J., Qiu, X., & Yang, Z. (2020). Five-year climatology of local convections in the Dabie mountains. Atmosphere, 11(11), 1246. doi:10.3390/atmos11111246.

[32] Hou, Y., & Dai, Y. (2024). Spatial Configuration and Sustainable Conservation of Ecotourism Resources in the Dabie Mountains, Eastern China, Using an Ecosystem Services Model. Diversity, 16(12), 782. doi:10.3390/d16120782.

[33] Qin, X., Li, J., & Li, N. (2025). Fine-Scale Spatiotemporal Distribution Characteristics of Precipitation in the Dabie Mountains Region. Journal of Applied Meteorology and Climatology, 64(12), 1803–1817. doi:10.1175/JAMC-D-25-0014.1.

[34] Yang, T., Wu, F., Luo, M., Xiong, J., Nie, X., Cao, F., Ruan, Y., Li, F., Huang, W., Liang, T., & Yang, Y. (2024). Accumulation Pattern and Potential Ecological Risk of Heavy Metals in Topsoil as Affected by Diverse Sources in Different Ecosystems in Western Dabie Mountain. Forests, 15(7), 1116. doi:10.3390/f15071116.

[35] Li, G., Yang, T., Chen, R., Dong, H., Wu, F., Zhan, Q., Huang, J., Luo, M., & Wang, L. (2025). Experimental study on in-situ simulation of rainfall-induced soil erosion in forest lands converted to cash crop areas in Dabie Mountains. PLoS ONE, 20(2 February), 317889. doi:10.1371/journal.pone.0317889.

[36] Zhu, Y., Du, C., Sun, L., Liu, X., Jamshidi, A. H., & Zhang, S. (2024). Impacts of intercropping tea trees under forest on soil water infiltration in the northern of Dabie Mountains. Nongye Gongcheng Xuebao/Transactions of the Chinese Society of Agricultural Engineering, 40(19), 72–82. doi:10.11975/j.issn.1002-6819.202403063.

[37] Zhu, Y., Sun, L., Jamshidi, A. H., Liu, X., Zheng, Y., & Fan, Z. (2025). Effect of forest conversion on soil water infiltration in the Dabie mountainous area, China. Journal of Hydrology: Regional Studies, 59, 102351. doi:10.1016/j.ejrh.2025.102351.

[38] Loess Plateau SubCenter (2026). National Earth System Science Data Center, National Science & Technology Infrastructure of China. Available online: http://loess.geodata.cn (accessed on May 2026)

[39] Karra, K., Kontgis, C., Statman-Weil, Z., Mazzariello, J. C., Mathis, M., & Brumby, S. P. (2021). Global Land Use/Land Cover with Sentinel 2 and Deep Learning. International Geoscience and Remote Sensing Symposium (IGARSS), 2021-July, 4704–4707. doi:10.1109/IGARSS47720.2021.9553499.

[40] Xie, W.-F., Li, J.-K., Peng, K., Zhang, K., & Ullah, Z. (2024). The Application of Local Moran's I and Getis–Ord Gi* to Identify Spatial Patterns and Critical Source Areas of Agricultural Nonpoint Source Pollution. Journal of Environmental Engineering, 150(5), 4024011. doi:10.1061/joeedu.eeeng-7585.

[41] Boubekraoui, H., Maouni, Y., Ghallab, A., Draoui, M., & Maouni, A. (2023). Spatio-temporal analysis and identification of deforestation hotspots in the Moroccan western Rif. Trees, Forests and People, 12, 100388. doi:10.1016/j.tfp.2023.100388.

[42] Nie, Q., Wu, G., Li, L., Man, W., Ma, J., Bao, Z., Luo, L., & Li, H. (2024). Exploring scaling differences and spatial heterogeneity in drivers of carbon storage Changes: A comprehensive geographic analysis framework. Ecological Indicators, 165, 112193. doi:10.1016/j.ecolind.2024.112193.

[43] Wang, J. F., Li, X. H., Christakos, G., Liao, Y. L., Zhang, T., Gu, X., & Zheng, X. Y. (2010). Geographical detectors-based health risk assessment and its application in the neural tube defects study of the Heshun Region, China. International Journal of Geographical Information Science, 24(1), 107–127. doi:10.1080/13658810802443457.

[44] Wang, J. F., Zhang, T. L., & Fu, B. J. (2016). A measure of spatial stratified heterogeneity. Ecological Indicators, 67, 250–256. doi:10.1016/j.ecolind.2016.02.052.

[45] Wu, Z., Liu, Y., Li, G., Han, Y., Li, X., & Chen, Y. (2022). Influences of Environmental Variables and Their Interactions on Chinese Farmland Soil Organic Carbon Density and Its Dynamics. Land, 11(2), 208. doi:10.3390/land11020208.

[46] Chen, L., & Shi, L. (2024). Differences in urban–rural gradient and driving factors of PM2.5 concentration in the Zhengzhou Metropolitan Area. Air Quality, Atmosphere and Health, 17(10), 2187–2201. doi:10.1007/s11869-024-01564-9.

[47] Wang, J., & Xu, C. (2017). Geodetector: Principle and prospective. Dili Xuebao/Acta Geographica Sinica, 72(1), 116–134. doi:10.11821/dlxb201701010.

[48] Song, Y., Wang, J., Ge, Y., & Xu, C. (2020). An optimal parameters-based geographical detector model enhances geographic characteristics of explanatory variables for spatial heterogeneity analysis: cases with different types of spatial data. GIScience and Remote Sensing, 57(5), 593–610. doi:10.1080/15481603.2020.1760434.

[49] Wu, J. (2004). Effects of changing scale on landscape pattern analysis: Scaling relations. Landscape Ecology, 19(2), 125–138. doi:10.1023/B:LAND.0000021711.40074.ae.

[50] Arrouays, D., McBratney, A. B., Minasny, B., Hempel, J. W., Heuvelink, G. B. M., McMillan, R. A., Hartemink, A. E., Lagacherie, P., & McKenzie, N. J. (2013). GlobalSoilMap. Basis for the global spatial soil information system. CRC Press, Florida, United States.

[51] Li, A. W., Ran, M., Song, L. Y., Xue, J. L., Zhang, Y. Y., Li, C. J., Deng, Q., Fang, H. Y., Dai, T. F., & Li, Q. Q. (2023). Spatial Distribution Characteristics and Influencing Factors of Cropland Topsoil Organic Carbon Content in the Sichuan Basin. Resources and Environment in the Yangtze Basin, 32(5), 1102–1112. doi:10.11870/cjlyzyyhj202305019.

[52] Jobbágy, E. G., & Jackson, R. B. (2000). The vertical distribution of soil organic carbon and its relation to climate and vegetation. Ecological Applications, 10(2), 423–436. doi:10.1890/1051-0761(2000)010[0423:TVDOSO]2.0.CO;2.

[53] Jackson, R. B., Lajtha, K., Crow, S. E., Hugelius, G., Kramer, M. G., & Piñeiro, G. (2017). The Ecology of Soil Carbon: Pools, Vulnerabilities, and Biotic and Abiotic Controls. Annual Review of Ecology, Evolution, and Systematics, 48(1), 419–445. doi:10.1146/annurev-ecolsys-112414-054234.

[54] Rumpel, C., & Kögel-Knabner, I. (2011). Deep soil organic matter-a key but poorly understood component of terrestrial C cycle. Plant and Soil, 338(1), 143–158. doi:10.1007/s11104-010-0391-5.

[55] Egli, M., Mirabella, A., & Sartori, G. (2008). The role of climate and vegetation in weathering and clay mineral formation in late Quaternary soils of the Swiss and Italian Alps. Geomorphology, 102(3–4), 307–324. doi:10.1016/j.geomorph.2008.04.001.

[56] Gami, S. K., Lauren, J. G., & Duxbury, J. M. (2009). Soil organic carbon and nitrogen stocks in Nepal long-term soil fertility experiments. Soil and Tillage Research, 106(1), 95–103. doi:10.1016/j.still.2009.10.003.

[57] Nielsen, D. R., & Bouma, J. (1985). Soil spatial variability: Proceedings of a workshop of the ISSS and the SSSA, Las Vegas, USA (Pudoc 296). Centre for Agricultural Publishing and Documentation, United States.

[58] Wilding, L. P. (1985). Spatial variability: its documentation, accommodation and implication to soil surveys. Soil Spatial Variability, 166–189.

[59] Schmidt, M. W. I., Torn, M. S., Abiven, S., Dittmar, T., Guggenberger, G., Janssens, I. A., Kleber, M., Kögel-Knabner, I., Lehmann, J., Manning, D. A. C., Nannipieri, P., Rasse, D. P., Weiner, S., & Trumbore, S. E. (2011). Persistence of soil organic matter as an ecosystem property. Nature, 478(7367), 49–56. doi:10.1038/nature10386.

[60] Grüneberg, E., Schöning, I., Hessenmöller, D., Schulze, E. D., & Weisser, W. W. (2013). Organic layer and clay content control soil organic carbon stocks in density fractions of differently managed German beech forests. Forest Ecology and Management, 303, 1–10. doi:10.1016/j.foreco.2013.03.014.

[61] Niu, X., Liu, C., Jia, X., & Zhu, J. (2021). Changing soil organic carbon with land use and management practices in a thousand-year cultivation region. Agriculture, Ecosystems and Environment, 322, 107639. doi:10.1016/j.agee.2021.107639.

[62] Yang, X., Xu, J., Wang, H., Quan, H., Yu, H., Luan, J., Wang, D., Li, Y., & Lv, D. (2024). Vertical distribution characteristics of soil organic carbon and vegetation types under different elevation gradients in Cangshan, Dali. PeerJ, 12, 16686. doi:10.7717/peerj.16686.

[63] Batjes, N. H. (2014). Total carbon and nitrogen in the soils of the world. European Journal of Soil Science, 65(1), 10–21. doi:10.1111/ejss.12114_2.

[64] Mishra, U., Lal, R., Slater, B., Calhoun, F., Liu, D., & Van Meirvenne, M. (2009). Predicting Soil Organic Carbon Stock Using Profile Depth Distribution Functions and Ordinary Kriging. Soil Science Society of America Journal, 73(2), 614–621. doi:10.2136/sssaj2007.0410.

[65] Zhang, Z., Huang, X., & Zhou, Y. (2020). Spatial heterogeneity of soil organic carbon in a karst region under different land use patterns. Ecosphere, 11(3), 3077. doi:10.1002/ecs2.3077.

[66] Zhou, J., Wang, Y., Tong, Y., Sun, H., Zhao, Y., & Zhang, P. (2023). Regional spatial variability of soil organic carbon in 0–5 m depth and its dominant factors. Catena, 231, 107326. doi:10.1016/j.catena.2023.107326.

[67] Deng, L., Liu, G. bin, & Shangguan, Z. ping. (2014). Land-use conversion and changing soil carbon stocks in China's "Grain-for-Green" Program: A synthesis. Global Change Biology, 20(11), 3544–3556. doi:10.1111/gcb.12508.

[68] Conant, R. T., Cerri, C. E. P., Osborne, B. B., & Paustian, K. (2017). Grassland management impacts on soil carbon stocks: A new synthesis: A. Ecological Applications, 27(2), 662–668. doi:10.1002/eap.1473.

[69] Kayranli, B., Scholz, M., Mustafa, A., & Hedmark, Å. (2010). Carbon storage and fluxes within freshwater wetlands: A critical review. Wetlands, 30(1), 111–124. doi:10.1007/s13157-009-0003-4.

[70] West, T. O., & Post, W. M. (2002). Soil Organic Carbon Sequestration Rates by Tillage and Crop Rotation. Soil Science Society of America Journal, 66(6), 1930–1946. doi:10.2136/sssaj2002.1930.

[71] Ogle, S. M., Breidt, F. J., & Paustian, K. (2005). Agricultural management impacts on soil organic carbon storage under moist and dry climatic conditions of temperate and tropical regions. Biogeochemistry, 72(1), 87–121. doi:10.1007/s10533-004-0360-2.

[72] Tsozué, D., Nghonda, J. P., Tematio, P., & Basga, S. D. (2019). Changes in soil properties and soil organic carbon stocks along an elevation gradient at Mount Bambouto, Central Africa. Catena, 175, 251–262. doi:10.1016/j.catena.2018.12.028.

[73] Zhang, Y., Ai, J., Sun, Q., Li, Z., Hou, L., Song, L., Tang, G., Li, L., & Shao, G. (2021). Soil organic carbon and total nitrogen stocks as affected by vegetation types and altitude across the mountainous regions in the Yunnan Province, south-western China. Catena, 196, 104872. doi:10.1016/j.catena.2020.104872.

[74] Phillips, J., Ramirez, S., Wayson, C., & Duque, A. (2019). Differences in carbon stocks along an elevational gradient in tropical mountain forests of Colombia. Biotropica, 51(4), 490–499. doi:10.1111/btp.12675.

[75] Girardin, C. A. J., Malhi, Y., Aragão, L. E. O. C., Mamani, M., Huaraca Huasco, W., Durand, L., Feeley, K. J., Rapp, J., Silva-Espejo, J. E., Silman, M., Salinas, N., & Whittaker, R. J. (2010). Net primary productivity allocation and cycling of carbon along a tropical forest elevational transect in the Peruvian Andes. Global Change Biology, 16(12), 3176–3192. doi:10.1111/j.1365-2486.2010.02235.x.

[76] He, P., Lu, J., Ren, Y., Li, J., Hou, L., Deng, X., Gao, T., & Cheng, F. (2023). Altitude and slope aspects as the key factors affecting the change of C:N:P stoichiometry in the leaf-litter-soil system of alpine timberline ecotones of the Sygera Mountains in Southeast Tibet, China. Geoderma Regional, 32, 602. doi:10.1016/j.geodrs.2022.e00602.

[77] Zhang, X., Li, X., Ji, X., Zhang, Z., Zhang, H., Zha, T., & Jiang, L. (2021). Elevation and total nitrogen are the critical factors that control the spatial distribution of soil organic carbon content in the shrubland on the Bashang Plateau, China. Catena, 204, 105415. doi:10.1016/j.catena.2021.105415.

[78] Song, X., Cao, M., Li, J., Kitching, R. L., Nakamura, A., Laidlaw, M. J., Tang, Y., Sun, Z., Zhang, W., & Yang, J. (2021). Different environmental factors drive tree species diversity along elevation gradients in three climatic zones in Yunnan, southern China. Plant Diversity, 43(6), 433–443. doi:10.1016/j.pld.2021.04.006.

[79] Xing, W., Lu, X., Ying, J., Lan, Z., Chen, D., & Bai, Y. (2022). Disentangling the effects of nitrogen availability and soil acidification on microbial taxa and soil carbon dynamics in natural grasslands. Soil Biology and Biochemistry, 164, 108495. doi:10.1016/j.soilbio.2021.108495.

[80] Sollins, P., & Gregg, J. W. (2017). Soil organic matter accumulation in relation to changing soil volume, mass, and structure: Concepts and calculations. Geoderma, 301, 60–71. doi:10.1016/j.geoderma.2017.04.013.

[81] Davidson, E. A., Trumbore, S. E., & Amundson, R. (2000). Soil warming and organic carbon content. Nature, 408(6814), 789–790. doi:10.1038/35048672.

[82] Chen, Q., Niu, B., Hu, Y., Luo, T., & Zhang, G. (2020). Warming and increased precipitation indirectly affect the composition and turnover of labile-fraction soil organic matter by directly affecting vegetation and microorganisms. Science of the Total Environment, 714, 136787. doi:10.1016/j.scitotenv.2020.136787.

[83] Zhang, L., Zheng, Q., Liu, Y., Liu, S., Yu, D., Shi, X., Xing, S., Chen, H., & Fan, X. (2019). Combined effects of temperature and precipitation on soil organic carbon changes in the uplands of eastern China. Geoderma, 337, 1105–1115. doi:10.1016/j.geoderma.2018.11.026.

[84] Zhuo, Z., Chen, Q., Zhang, X., Chen, S., Gou, Y., Sun, Z., Huang, Y., & Shi, Z. (2022). Soil organic carbon storage, distribution, and influencing factors at different depths in the dryland farming regions of Northeast and North China. Catena, 210, 105934. doi:10.1016/j.catena.2021.105934.

[85] Sun, T., Wang, Y., Hui, D., Jing, X., & Feng, W. (2020). Soil properties rather than climate and ecosystem type control the vertical variations of soil organic carbon, microbial carbon, and microbial quotient. Soil Biology and Biochemistry, 148, 107905. doi:10.1016/j.soilbio.2020.107905.